The current issue and full text archive of this journal is available on Emerald Insight at:
www.emeraldinsight.com/0961-5539.htm

Received 3 February 2014
Revised 28 April 2014
Accepted 8 June 2014

Non-Darcy natural convection flow for non-Newtonian nanofluid over cone saturated in porous medium with uniform heat and volume fraction fluxes

A. Chamkha
Manufacturing Engineering Department,
The Public Authority for Applied Education and Training, Shuweikh, Kuwait
S. Abbasbandy
Department of Mathematics, Imam Khomeini International University,
Ghazvin, Iran, and
A.M. Rashad
Department of Mathematics, Aswan University, Aswan, Egypt

Abstract

Purpose – The purpose of this paper is to investigate the effect of uniform lateral mass flux on non-Darcy natural convection of non-Newtonian fluid along a vertical cone embedded in a porous medium filled with a nanofluid.
Design/methodology/approach – The resulting governing equations are non-dimensionalized and transformed into a non-similar form and then solved numerically by Keller box finite-difference method.
Findings – A comparison with previously published works is performed and excellent agreement is obtained.
Research limitations/implications – The model used for the nanofluid incorporates the effects of Brownian motion and thermophoresis. It is assumed that the cone surface is preamble for possible nanofluid wall suction/injection, under the condition of uniform heat and nanoparticles volume fraction fluxes.
Originality/value – The effects of nanofluid parameters, Ergun number, surface mass flux and viscosity index are investigated on the velocity, temperature, and volume fraction profiles as well as the local Nusselt and Sherwood numbers.

Keywords Cone, Nanofluid, Brownian diffusion, Natural convection, Porousmedia, Thermophoresis
Paper type Research paper

1. Introduction

Convective flow in porous media has been widely studied in the recent years due to its wide applications in engineering as geophysical thermal and insulation engineering, the modeling of packed sphere beds, the cooling of electronic systems, groundwater hydrology, chemical catalytic reactors, ceramic processes, grain storage devices, fiber and granular insulation, petroleum reservoirs, coal combustors, ground water pollution and filtration processes, to name just a few of these applications. However, representative studies in this area may be found in the monographs by Vafai (2000),

The authors wish to express their very sincere thanks to the referees for their valuable comments and suggestions about this work.

0961-5539
DOI 10.1108/HFF-02-2014-0027

Pop and Ingham (2001), Ingham and Pop (2002), and Nield and Bejan (2006). Also, the study of laminar boundary layer flow heat transfer in non-Newtonian fluids from surfaces through porous media has received considerable attention in recent years because it is an important type of scientific and engineering applications such as aerodynamic extrusion of plastic sheets and fibers, drawing, annealing and tinning of copper wire, paper production, crystal growing and glass blowing. Such applications involve cooling of a molten liquid by drawing it in to a cooling system. Cheng *et al.* (1985) studied the problem of natural convection heat transfer of Darcian fluids over cone embedded in a fluid-saturated porous media. Chen and Chen (1988) studied the free convection of non-Newtonian fluids over vertical surface in porous media. Nakayama and Koyama (1991) investigated the natural convection over a non-isothermal body of arbitrary shape embedded in a porous medium. Pascal and Pascal (1997) reported the free convection in a non-Newtonian fluid saturated porous media with lateral mass flux. Yih (1998) considered the effect of uniform lateral mass flux on natural convection of non-Newtonian fluids over a cone in porous media. Gorla and Kumari (2000) employed a non-similar solution for mixed convection in non-Newtonian fluids along a wedge with variable surface heat flux.

On other side, nanofluids are prepared by dispersing solid nanoparticles in fluids such as water, oil, or ethylene glycol. These fluids represent an innovative way to increase thermal conductivity and, therefore, heat transfer. Unlike heat transfer in conventional fluids, the exceptionally high thermal conductivity of nanofluids provides for exceptional heat transfer, a unique feature of nanofluids. An innovative technique for improving heat transfer by using ultra fine solid particles in the fluids has been used extensively during the last several years. The term nanofluid refers to these kinds of fluids by suspending nano-scale particles in the base fluid and it has been introduced by Choi (1995). Buongiorno (2006) introduced a comprehensive survey of convective transport in nanofluids by studying the Brownian motion and the thermophoresis on the heat transfer characteristics. Duangthongsuk and Wongwises (2008) studied the influence of thermophysical properties of nanofluids on the convective heat transfer and summarized various models used in literature for predicting the thermophysical properties of nanofluids. Nield and Kuznetsov (2009) have studied the natural convection past a vertical plate in a porous medium saturated by a nanofluid with the effects of Brownian motion and thermophoresis. Gorla *et al.* (2011a) have discussed the mixed convective boundary layer flow over a vertical wedge embedded in a porous medium saturated with a nanofluid. Gorla *et al.* (2011b) have also presented a similarity analysis for the problem of steady boundary-layer flow of a nanofluid on an isothermal stretching circular cylindrical surface. The problem of natural convection boundary layer of a non-Newtonian fluid along a vertical cone embedded in a porous medium saturated with nanofluid was performed by Rashad *et al.* (2011). Khan and Aziz (2011) have studied the double-diffusive natural convective boundary layer flow over a vertical plate embedded in a porous medium saturated with a nanofluid. Uddin *et al.* (2012) have presented a numerical solution for free convection boundary layer flow of nanofluid from a heated upward facing horizontal flat plate embedded in a porous medium. Chamkha and Rashad (2012) reported the problem of natural convection from a vertical permeable cone in nanofluid saturated porous medium with uniform heat and volume fraction fluxes. Chamkha *et al.* (2012b) have analyzed the effect of radiation on boundary-layer flow of a nanofluid on a continuously moving or fixed permeable surface. Chamkha *et al.* (2012a, 2013a) investigated the effects of Brownian motion and thermophoresis on mixed convection over a wedge and cone embedded in a porous medium filled with a nanofluid. Chamkha *et al.* (2013b) have also examined the transient natural convection flow of a nanofluid over a vertical cylinder. RamReddy *et al.* (2013) investigated the double-diffusive mixed convection heat and mass transfer in the boundary layer region along a flat plate in a nanofluid. Murthy *et al.* (2013) have considered the magnetic effect on thermally stratified nanofluid saturated non-Darcy porous medium. Nadeem *et al.* (2014) obtained an analytical solution for stagnation-point flow of a Casson nanofluid over a stretching surface in the presence of convective boundary conditions. The problem of non-Darcy natural convection boundary-layer flow adjacent to a vertical cylinder embedded in a thermally stratified nanofluid saturated non-Darcy porous medium is presented Rashad *et al.* (2014). Nadeem and Haq (2014) have also studied the effect of thermal radiation for MHD boundary layer flow of a nanofluid past a stretching sheet with convective boundary conditions.

Hence, based on the above-mentioned investigations and applications, the present paper considers the effect of uniform lateral mass flux on non-Darcy natural convection boundary-layer flow of a non-Newtonian fluid over a permeable vertical cone embedded in a porous medium filled with nanofluid in the presence of effects of Brownian motion and thermophoresis. The cone surface maintained at uniform heat and nanoparticles volume fraction fluxes. The effects of nanoparticles Brownian motion and thermophoresis are included in the model. Numerical calculations were carried out for different values of the various dimensionless parameters controlling the flow regime, heat and mass transfer.

2. Governing equations

Consider the problem of mixed convection of a non-Newtonian fluid along a permeable vertical cone embedded in a porous medium filled with a nanofluid. The model used for the nanofluid incorporates the effects of Brownian motion and thermophoresis. The cone surface is maintained at a uniform heat flux and nanoparticles volume fraction flux q_w and m_w, respectively, and the ambient temperature and nanoparticles volume in the ambient medium are T_∞ and C_∞, respectively. Figure 1 shows the flow model and physical coordinate system. The origin of the coordinate system is placed at the vertex of the cone, where x and y are Cartesian coordinates measuring the distances along and normal to the surface of the cone, respectively. In the formulation of the present problem the following common assumptions are made: the flow is steady, incompressible, two-dimensional, convective fluid and the porous matrix is everywhere in local thermodynamic equilibrium and the fluid properties are assumed to be constant, except for density variations in the buoyancy term. Under these assumptions and the application of the Boussinesq and boundary-layer approximations, the governing conservation equations, with momentum equation based on the Darcy-Forchheimer model, can be written as Yih (1998):

$$\frac{\partial(ru)}{\partial x}+\frac{\partial(rv)}{\partial y}=0, \tag{1}$$

$$\frac{\partial u^n}{\partial y}+\frac{\rho_{f\infty}K^*}{\mu}\frac{\partial u^2}{\partial y}=\frac{(1-C_\infty)\rho_{f\infty}\cos\gamma\beta gK}{\mu}\frac{\partial T}{\partial y}-\frac{(\rho_p-\rho_{f\infty})\cos\gamma gK}{\mu}\frac{\partial C}{\partial y}, \tag{2}$$

$$u\frac{\partial T}{\partial x}+v\frac{\partial T}{\partial y}=\alpha\frac{\partial^2 T}{\partial y^2}+\tau\left[D_B\frac{\partial C}{\partial y}\frac{\partial T}{\partial y}+\left(\frac{D_T}{T_\infty}\right)\left(\frac{\partial T}{\partial y}\right)^2\right], \tag{3}$$

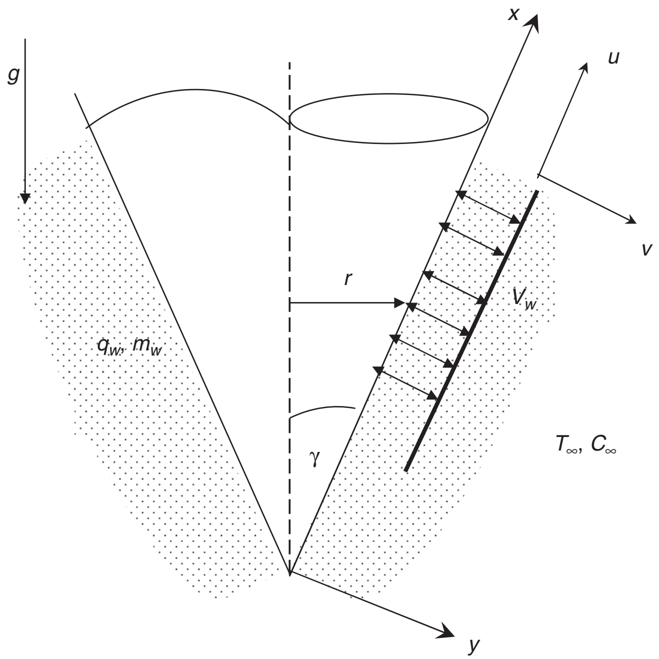

Figure 1.
Flow model and physical coordinate system

$$u\frac{\partial C}{\partial x}+v\frac{\partial C}{\partial y}=D_B\frac{\partial^2 C}{\partial y^2}+\left(\frac{D_T}{T_\infty}\right)\frac{\partial^2 T}{\partial y^2}, \tag{4}$$

where u, v, T and C are the x- and y- components of velocity, temperature and nanoparticles volume fraction, respectively. K, β, g, D_B and D_T are the permeability of the porous medium, volumetric expansion coefficient of the fluid, gravitational acceleration, Brownian diffusion coefficient and thermophoretic diffusion coefficient, respectively. K^*, γ, μ, ρ_f and ρ_p are the porous medium inertial coefficient, cone half angle, fluid viscosity, fluid density and nanoparticles mass density, respectively. $\alpha=k_m/(\rho c)_f$ and $\tau=(\rho c)_p/(\rho c)_f$ are the effective thermal diffusivity of porous medium and the ratio of heat capacities, respectively. k_m, $(\rho c)_f$ and $(\rho c)_p$ are effective thermal conductivity, heat capacity of the fluid and the effective heat capacity of nanoparticles material, respectively.

The boundary conditions suggested by the physics of the problem are given by:

$$y=0: v=V_w,\ -k_m\left(\frac{\partial T}{\partial y}\right)=q_w,\ -D_B\left(\frac{\partial C}{\partial y}\right)=m_w, \tag{5a}$$

$$y\to\infty: u=0, T=T_\infty, C=C_\infty, \tag{5b}$$

where V_w is the uniform transpiration velocity. We assume that the boundary layer is sufficiently thin in comparison with the local radius of the cone. The local radius to a point in the boundary layer, therefore, can be replaced by the radius of the cone r, i.e., $r=x\ \sin\gamma$. For the power law model of Christopher and Middlemann (1965) and Dharmadhikari and Kale (1985) proposed the following relationships for the permeability:

$$K = \frac{6}{25}\left(\frac{n\varepsilon}{3n+1}\right)^{n}\left(\frac{\varepsilon d}{3(1-\varepsilon)}\right)^{n+1}, \tag{6a}$$

$$K = \frac{2}{\varepsilon}\left(\frac{d\varepsilon^2}{8(1-\varepsilon)}\right)^{n+1}\frac{6n+1}{10n-3}\left(\frac{16}{75}\right)^{\frac{3(10n-3)}{10n+11}}, \tag{6b}$$

where d is the particle diameter and ε is the porosity. n the power law index. For the case $n<1$ the fluid represent the (shear-thinning or pseudo-plastic fluid), $n=1.0$ (Newtonian fluid) and $n>1$ (shear-thickening or dilatant fluid).

Introducing the stream function such that: $ru = \partial\psi/\partial y$, $rv = -\partial\psi/\partial x$ and invoking the following dimensionless variables:

$$\xi = \frac{2V_m x}{\alpha Ra_x^{1/3}}, \eta = \frac{y}{x}Ra_x^{1/3}, f(\xi,\eta) = \frac{\psi}{\alpha r Ra_x^{1/3}}, \theta(\xi,\eta) = \frac{(T-T_\infty)k_m Ra_x^{1/3}}{q_w x}, \phi = \frac{(T-T_\infty)D_B Ra_x^{1/3}}{m_w x} \tag{7}$$

into Equations (1)-(5) produce the following non-similar equations and boundary conditions:

$$nf'^{m-1}f'' + 2Rf'f'' = \theta' - Nr\phi', \tag{8}$$

$$\theta'' + Nb\phi'\theta' + \frac{3n+2}{2n+1}f\theta' - \frac{n}{2n+1}f'\theta + Nt\theta'^2 = \frac{n}{2n+1}\xi\left(f'\frac{\partial\theta}{\partial\xi} - \theta'\frac{\partial f}{\partial\xi}\right), \tag{9}$$

$$\frac{1}{Le}\phi'' + \frac{3n+2}{2n+1}f\phi' - \frac{n}{2n+1}f'\phi + \frac{Nt}{LeNb}\theta'' = \frac{n}{2n+1}\xi\left(f'\frac{\partial\phi}{\partial\xi} - \phi'\frac{\partial f}{\partial\xi}\right), \tag{10}$$

The dimensionless boundary conditions become:

$$\eta = 0 : f = -\frac{\xi}{4}, \theta' = -1, \phi' = -1, \tag{11a}$$

$$\eta \to \infty : \theta = 0, \phi = 0, \tag{11b}$$

where a prime denotes partial differentiation with respect to η and:

$$Ra_x = (x/\alpha)^{3n/(2n+1)}\left\{(1-C_\infty)\rho_{f\infty} g\cos\gamma\beta K q_w x/(\mu K_m)\right\}^{3/(2n+1)}$$
$$R^* = (\rho_{f\infty} bK/\mu)(\alpha/x)^{2-n}(Ra_x)^{4-2n/3}$$

$$Nr = \frac{(\rho_p-\rho_{f\infty})m_w k_m Ra_x^{1/3}}{(1-C_\infty)\rho_{f\infty}\beta q_w D_B}, Nb = \frac{(\rho c)_p m_w x}{(\rho c)_f \alpha Ra_x^{1/3}}, Nt = \frac{(\rho c)_p D_T q_w x}{(\rho c)_f \alpha T_\infty k_m Ra_x^{1/3}}, Le = \alpha/D_B, \tag{12}$$

are the generalized modified Rayleigh number, non-Darcy parameter, buoyancy ratio, Brownian motion parameter , thermophoresis parameter and Lewis number, respectively. In the above equations, It is noted that the mass flux parameter $\xi > 0$ for $V_w > 0$ corresponds to the case of fluid injection and $\xi < 0$ for $V_w < 0$ corresponds to the case of fluid suction or withdrawal. Also, it is important to notice that most nanofluids examined to date have large values for the Lewis number $Le > 1$ (see Nield and Kuznetsov (2009)). For water nanofluids at room temperature with nanoparticles of 1-100 nm diameters, the Brownian diffusion coefficient D_B ranges from 4×10^{-12} to 4×10^{-4} m^2/s. Furthermore, the ratio of the Brownian diffusivity coefficient to the thermophoresis coefficient for particles with diameters of 1-100 nm can be varied in the ranges of 0.02-2.0 for alumina, and from 2 to 20 for copper nanoparticles (see Buongiorno (2006) for details). Hence, the variation of the non-dimensional parameters of nanofluids in the present study is considered to vary in the mentioned range.

Of special significance for this problem are the local Nusselt and Sherwood numbers. These physical quantities can be defined as:

$$Nu_x Ra_x^{-1/3} = \frac{1}{\theta(\xi, 0)}, \quad (13)$$

$$Sh_x Ra_x^{-1/3} = \frac{1}{\phi(\xi, 0)} \quad (14)$$

3. Numerical method and validation

The governing Equations (8)-(10) with the boundary conditions (11) are non-linear partial differential equations. The system of Equations (8)-(10) are solved numerically using an implicit finite-difference scheme known as the Keller box method as described by Cebeci and Bradshaw (1984). For solving the non-linear system of equations in the Keller box method, we used the Newton-Armijo method (1995) with a reduced factor 0.0001. The computations were carried out with $\Delta\eta = 0.01$ (uniform grids). The value of $\eta_\infty = 8$ was found to be sufficiently enough to obtain the accuracy of $|f''(0)| < 10^{-6}$. In order to access the accuracy of the numerical results, we have compared the results obtained by this numerical method with the previously published work of Cheng *et al.* (1985) and Yih (1998) for various values of n for Darcian flow ($R = 0$) in the absence of nanoparticles volume fraction parameters ($Nr = Nb = Nt = 0$). These comparisons are presented in Tables I and II. It can be seenfrom these tables that excellent agreement between the results exists. These favorable comparisons lend confidence in the numerical results to be reported in the next section.

n	Cheng *et al.* (1985)	Yih (1998)	Present work
0.5	–	1.1358	1.13577
0.8	–	1.0839	1.08387
1.0	1.0562	1.0564	1.05636
1.5	–	0.9871	1.00736
2.0	–	0.9760	0.975992

Notes: $R = Nr = Nb = Nt = 0$

Table I.
Comparison of θ (0,0) for a vertical cone

4. Results and discussion

In this section, a representative set of numerical results for the dimensionless velocity, temperature, and nano-particle volume fraction profiles as well as the local Nusselt number and the local Sherwood number is presented graphically in Figures 2-16. These results illustrate the effects of the power-law index parameter n, non-Darcy

Table II.
Comparison of θ (ξ, 0) for a vertical cone

ξ	Yih (1998) $n=0.5$	Yih (1998) $n=2$	Present work $n=0.5$	Present work $n=2$
−4	0.4896	0.4453	0.488004	0.45785
−2	0.7963	0.6577	0.795603	0.65813
0	1.1358	0.9760	1.13577	0.975992
2	1.4221	1.3908	1.4029	1.38949
4	1.6672	1.8758	1.4039	1.82448

Notes: $R=Nr=Nb=Nt=0$

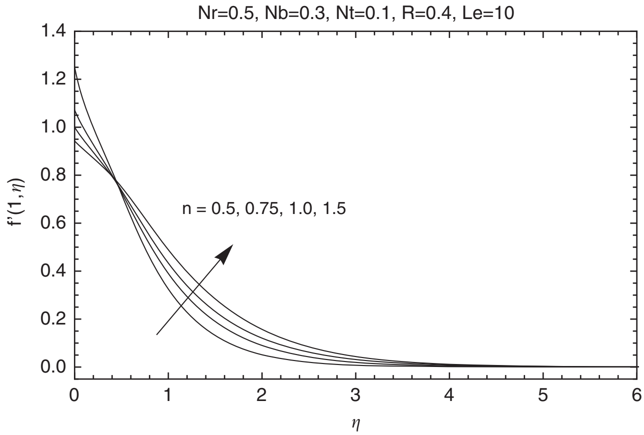

Figure 2.
Effect of power law index n on the velocity profiles

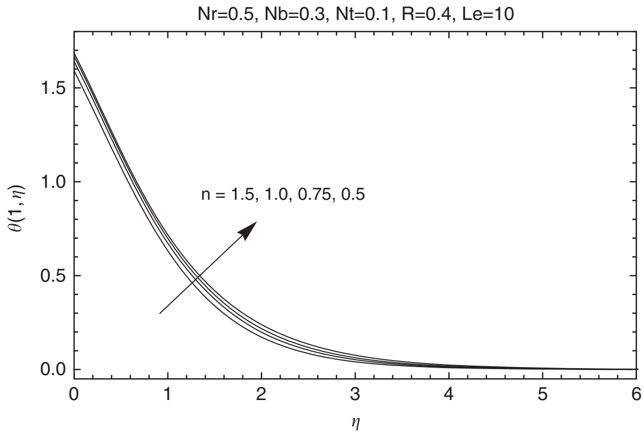

Figure 3.
Effect of power law index n on the temperature profiles

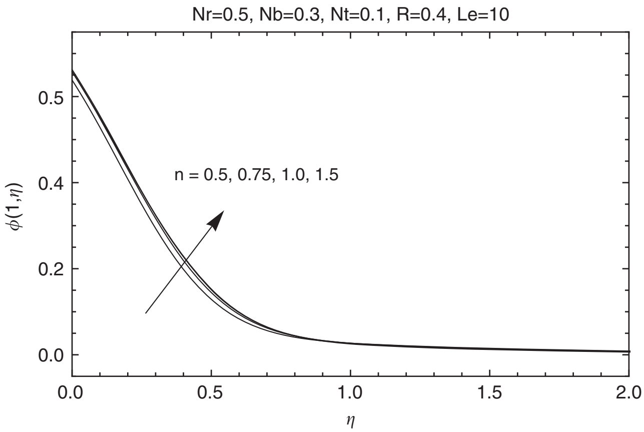

Figure 4.
Effect of power law index n on the volume fraction profiles

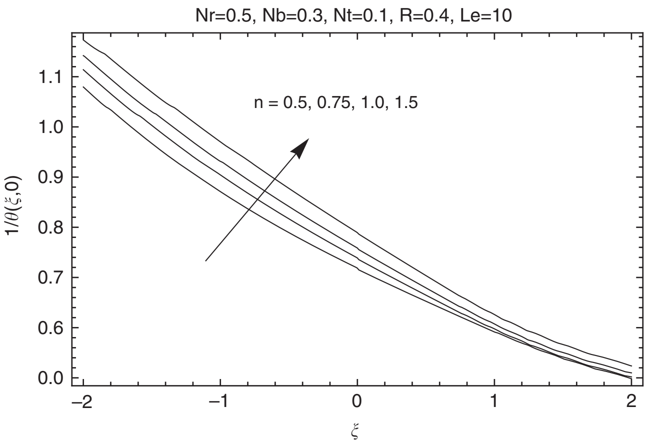

Figure 5.
Effect of power law index n on the local Nusselt number

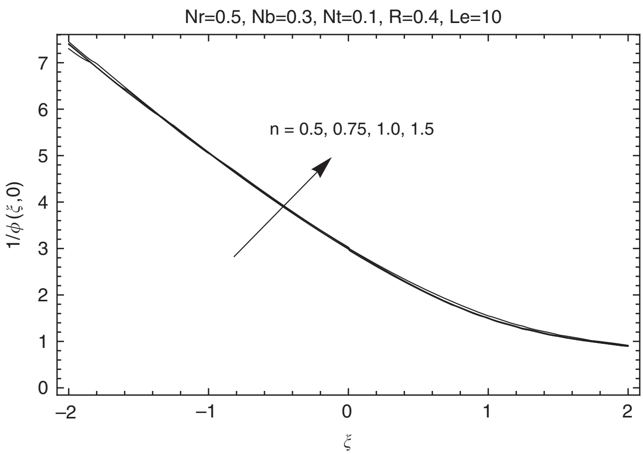

Figure 6.
Effect of power law index n on the local Sherwood number

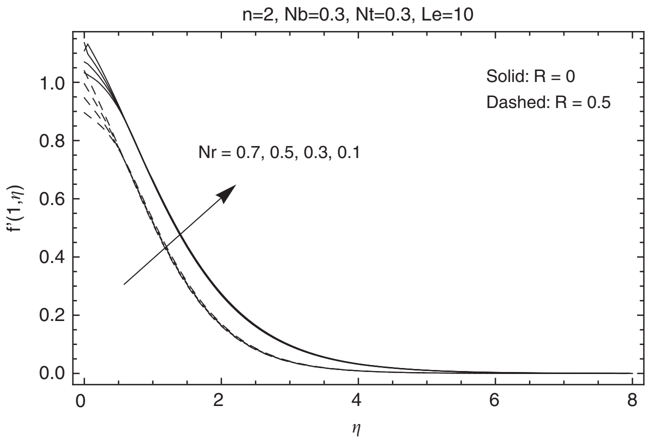

Figure 7.
Effects of the buoyancy ratio Nr and non-Darcy parameter R on the velocity profiles

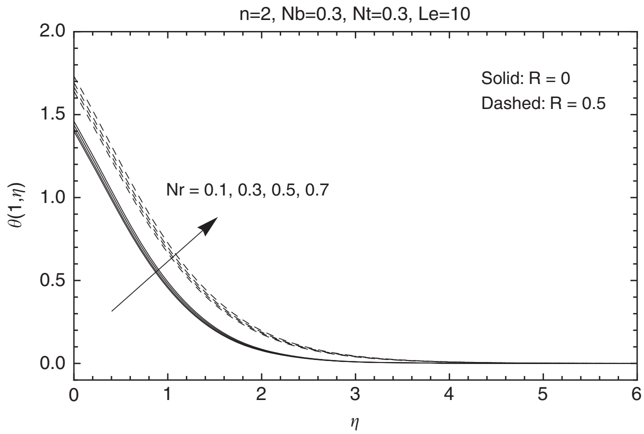

Figure 8.
Effects of the buoyancy ratio Nr and non-Darcy parameter R on the temperature profiles

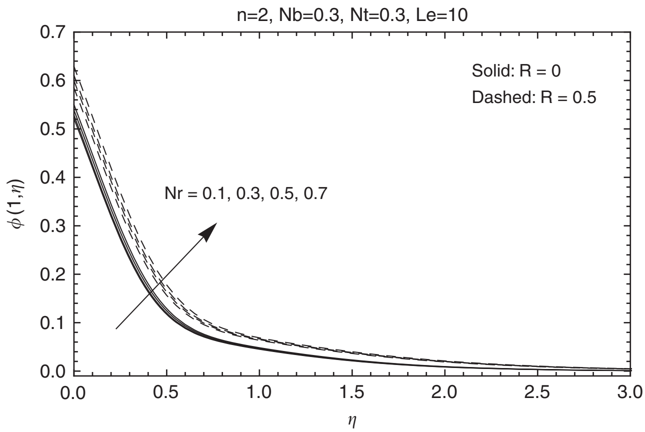

Figure 9.
Effects of the buoyancy ratio Nr and non-Darcy parameter R on the volume fraction profiles

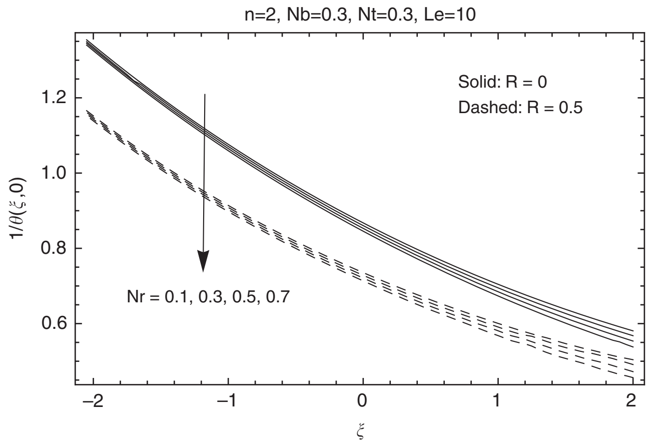

Figure 10.
Effects of the buoyancy ratio Nr and non-Darcy parameter R on the local Nusselt number

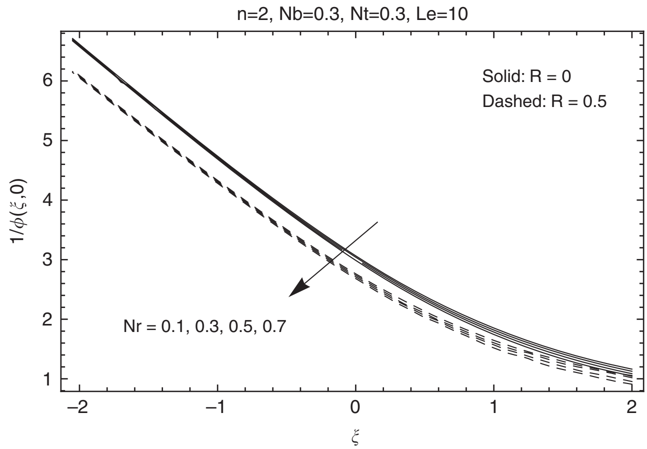

Figure 11.
Effects of the buoyancy ratio Nr and non-Darcy parameter R on the local Sherwood number

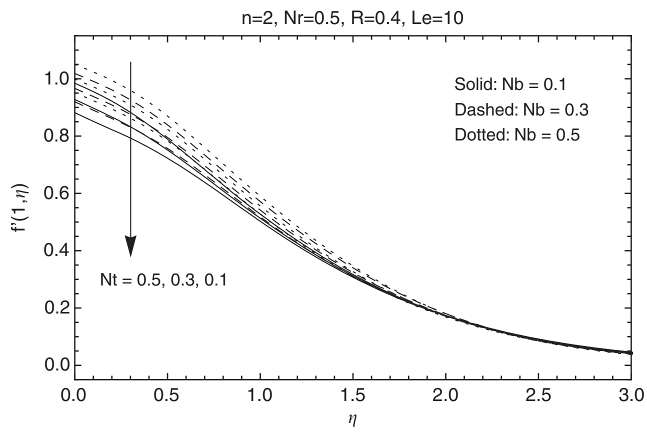

Figure 12.
Effects of brownian motion parameter Nb and thermophoresis parameter Nt on the velocity profiles

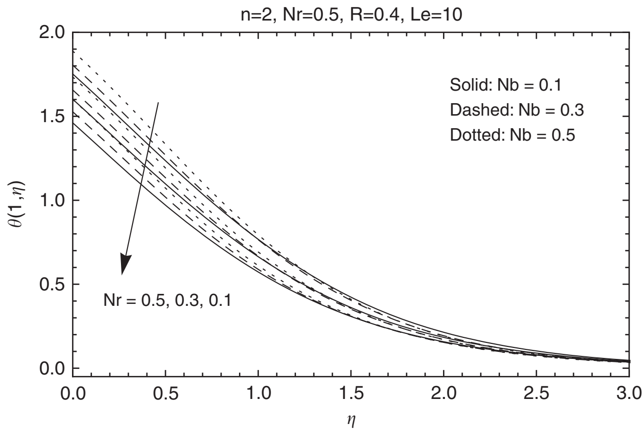

Figure 13. Effects of brownian motion parameter Nb and thermophoresis parameter Nt on the temperature profiles

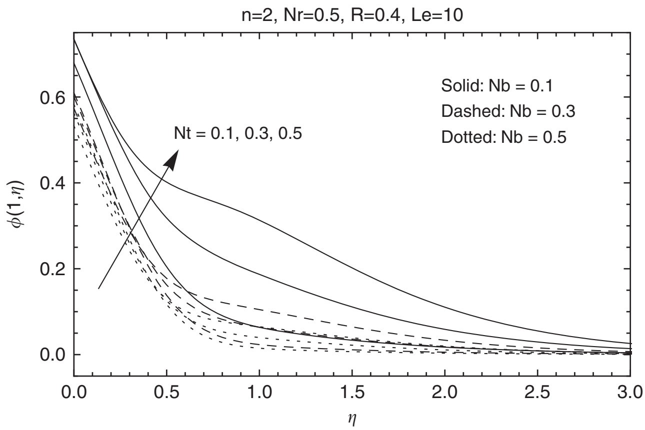

Figure 14. Effects of brownian motion parameter Nb and thermophoresis parameter Nt on the volume fraction profiles

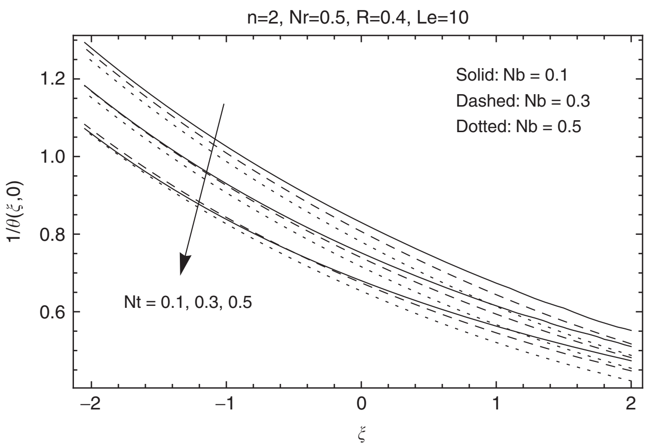

Figure 15. Effects of brownian motion parameter Nb and thermophoresis parameter Nt on the local Nusselt number

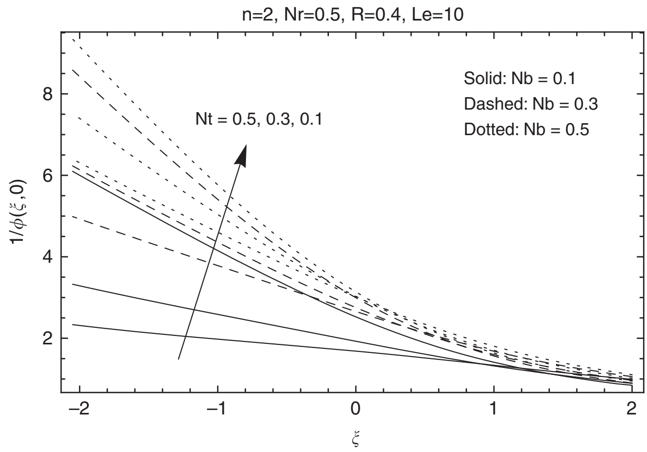

Figure 16.
Effects of brownian motion parameter Nb and thermophoresis parameter Nt on the local Sherwood number

parameter *R*, buoyancy ratio *Nr*, Brownian motion parameter *Nb* and thermophoresis parameter *Nt* on the solutions for different values of mass flux parameter ξ (suction/injection cases).

Figures 2-4 display the effect of power law index parameter n on the dimensionless velocity f', temperature θ and volume fraction ϕ profiles, respectively. It is mentioned that the power-law fluid viscosity indices $n = 0.5, 0.75$ (shear-thinning or pseudo-plastic fluid), $n = 1.0$ (Newtonian fluid) and $n = 1.5$ (shear-thickening or dilatant fluid). However, it is clearly seen that as the power-law index n increases, both the volume fraction and temperature profiles increase, while the slip velocity at the cone surface decreases. In addition, the non-Newtonian fluid with a higher power-law index has a greater thermal boundary layer thickness and a greater volume fraction boundary-layer thickness. Moreover, increasing the power-law index leads to decelerate the flow and increase either the thermal or the volume fraction boundary layer thicknesses.

Figures 5 and 6 indicate the variations of the power law index n on the local Nusselt number $Nu_x Ra_x^{-1/3}$, and the local Sherwood number $Sh_x Ra_x^{-1/3}$, for various values of the power-law index n and mass flux parameter ξ, respectively. As shown from the definitions of $Nu_x Ra_x^{-1/3}$, and $Sh_x Ra_x^{-1/3}$, they are directly proportional to $1/\theta(\xi,0)$ and $1/\phi(\xi,0)$, respectively. From these figures, it is noticed that the increasing the power-law index n leads to raise both the local Nusselt and Sherwood numbers. On contrast, as the mass flux parameter ξ increases from minus values (suction case) to positive values (injection case), both of the heat transfer rate (local Nusselt number) and the mass transfer rate (local Sherwood number) decrease. Moreover, the maximum heat and mass transfer rate corresponds to the minimum ξ. This behavior is especially clear in the large suction case.

Figures 7-9 present the effects of the buoyancy ratio *Nr* and non-Darcy parameter *R* on the velocity, temperature and volume fraction profiles. In general, increases in the value of *Nr* have the prevalent to cause more induced flow along the cone surface. This behavior in the flow velocity is accompanied by increases in the fluid temperature and volume fraction species as well as slight increases in the thermal and volume fraction boundary layers as *Nr* increases. Moreover, it is observed that, as the non-Darcy parameter *R* increases, both of the temperature and the nanoparticles volume fraction profiles increase, while the velocity profiles within the boundary layer decrease. This in fact is the non-Darcy parameter that represents the Forchheimer effect which is the second-order nonlinear porous medium inertial resistance. This means increasing inertial effects the Forchheimer drag will be dominant, and then causes a strong deceleration in the flow in the boundary layer. On other hand, Figures 10 and 11 depict the effects of the buoyancy ratio *Nr* and non-Darcy parameter *R* on the local Nusselt number $1/\theta(\xi,0)$, and local Sherwood number $1/\phi(\xi,0)$, respectively. As mentioned above, that the increases in the nanofluid temperature and volume fraction as *Nr* increases. This causes the heat and volume fraction fluxes to reduce yielding corresponding reduction in both the local Nusselt and Sherwood numbers. Furthermore, The same effect is occurred with the non-Darcy parameter *R* on $1/\theta(\xi,0)$ and $1/\phi(\xi,0)$. The reason for this trend happened because the nanofluid motion in the boundary layer is decelerated causing a decrease in the momentum boundary layer in the presence of Forchheimer effect and hence, enhancement in the thermal and nanoparticle concentration boundary layer thickness. Consequently, the heat and mass transfer rates decrease with increasing values of *R*.

Finally, the effects of Brownian motion parameter *Nb* and thermophoresis parameter *Nt* on the velocity, temperature and volume fraction profiles are shown in Figures 12-14. It is observed that the velocity profiles near the surface increase strongly with the increase of Brownian motion parameter *Nb* while the opposite behavior happens with the volume fraction. This increasing in the flow velocity near the surface is achieved at the expense of significant enhancement in the fluid temperature. Also, it is noticed that increasing the thermophoresis parameter *Nt* has a tendency to retard the flow and to decrease in the temperature profiles. This, in turn, produces a reduction in the fluid temperature and a rises in the volume fraction profiles. Furthermore, Figures 15 and 16 display the effects of Brownian motion parameter *Nb* and thermophoresis parameter *Nt* on the local Nusselt number $1/\theta(\xi,0)$ and local Sherwood number $1/\phi(\xi,0)$, respectively. In nanofluid systems, owing to the size of the nanoparticles, Brownian motion takes place, and this can enhance the heat transfer properties. This is due to the fact that the Brownian diffusion promotes heat conduction. The nanoparticles rise at the cone surface area for heat transfer. A nanofluid is a two phase fluid where the nanoparticles move randomly and raise the energy exchange rates. However, the Brownian motion decreases nanoparticles diffusion. The enhancement in the local Sherwood number as Brownian motion parameter *Nb* changes is relatively small. Therefore, as noted before that, the effect of the Brownian motion parameter *Nb* is to enhance the temperature profiles while its volume fraction reduces. This causes a decrease in the local Nusselt number and an increase in the local Sherwood number. On the other side, it is observed that the thermophoresis parameter *Nt* exhibits in thermal and nanoparticles boundary layer equations. This is formation with the well known fact that it is coupled with the temperature function and plays a strong role in determining the diffusion of heat and nanoparticles in the boundary layer. Thus, the increasing the thermophoresis parameter *Nt* causes a reduction in both the local Nusselt number and local Sherwood numbers.

4. Conclusions

The effect of uniform lateral mass flux on non-Darcy natural convection of non-Newtonian fluid along a vertical cone embedded in a porous medium filled with a nanofluid is investigated. The model used for the nanofluid incorporates the effects of Brownian motion and thermophoresis. The cone surface is assumed to be permeable for possible nanofluid wall suction/injection, under the condition of uniform heat and nanoparticles volume fraction fluxes. The resulting governing equations are non-dimensionalized and transformed into a non-similar form and then solved numerically by Keller box finite-difference method. A comparison with previously published works is performed and excellent agreement is obtained. Numerical results for the velocity, temperature, and volume fraction profiles as well as the local Nusselt number and the local Sherwood number were reported graphically. It was concluded that both the local Nusselt and Sherwood numbers rose due to increase in the power-law fluid index, whereas the reverse trend is happened with increase the lateral mass flux parameter. Also, it was found that as the buoyancy ratio, non-Darcy parameter or thermophoresis parameter increased, both the local Nusselt and Sherwood numbers reduced. Finally, the increasing of Brownian motion parameter leads to enhance the local Sherwood number and to reduce the local Nusselt number.

References

Buongiorno, J. (2006), "Convective transport in nanofluids", *ASME J. Heat Transfer*, Vol. 128 No. 3, pp. 240-250.

Cebeci, T. and Bradshaw, P. (1984), *Physical and Computational Aspects of Convective Heat Transfer*, 2nd ed., Springer-Verlag, New York, NY.

Chamkha, A.J. and Rashad, A.M. (2012), "Natural convection from a vertical permeable cone in nanofluid saturated porous media for uniform heat and nanoparticles volume fraction fluxes", *Int. J. Numerical Methods for Heat and Fluid Flow*, Vol. 22 No. 8, pp. 1073-1085.

Chamkha, A.J., Abbasbandy, S., Rashad, A.M. and Vajravelu, K. (2012a), "Radiation effects on mixed convection over a wedge embedded in a porous medium filled with a nanofluid", *Transport in Porous Medium*, Vol. 91 No. 1, pp. 261-279.

Chamkha, A.J., Abbasbandy, S., Rashad, A.M. and Vajravelu, K. (2013a), "Radiation effects on mixed convection about a cone embedded in a porous medium filled with a nanofluid", *Meccanica*, Vol. 48 No. 2, pp. 275-285.

Chamkha, A.J., Modather, M., EL-Kabeir, S.M.M. and Rashad, A.M. (2012b), "Radiative effects on boundary-layer flow of a nanofluid on a continuously moving or fixed permeable surface", *Recent Patents on Mechanical Engineering*, Vol. 5 No. 3, pp. 176-183.

Chamkha, A.J., Rashad, A.M. and Aly, A.M. (2013b), "Transient natural convection flow of a nanofluid over a vertical cylinder", *Meccanica*, Vol. 48 No. 1, pp. 71-81.

Chen, H.T. and Chen, C.K. (1988), "Free convection of non-newtonian fluids along a vertical plate embedded in a porous medium", *Transactions of ASME, Journal of Heat Transfer*, Vol. 110 No. 1, pp. 257-260.

Cheng, P., Le, T.T. and Pop, I. (1985), "Natural convection of a darcian fluid about a cone", *Int. Comm. Heat Mass Transfer*, Vol. 12 No. 6, pp. 705-717.

Choi, S.U.S. (1995), "Enhancing thermal conductivity of fluids with nanoparticle", in Siginer, D.A. and Wang, H.P. (Eds), *Developments and Applications of Non-Newtonian Flows*, ASME Press, New York, NY, Vol. /MD 231/66, pp. 99-105.

Christopher, R.H. and Middleman, S. (1965), "Power-law flow through a packed tube", *I & EC Fundamentals*, Vol. 4, pp. 422-426.

Dharmadhikari, R.V. and Kale, D.D. (1985), "Flow of non-newtonian fluids through porous media", *Chemical Eng. Sci.*, Vol. 40 No. 3, pp. 527-529.

Duangthongsuk, W. and Wongwises, S. (2008), "Effect of thermophysical properties models on the predicting of the convective heat transfer coefficient for low concentration nanofluid", *International Communications in Heat and Mass Transfer*, Vol. 35 No. 10, pp. 1320-1326.

Gorla, R.S.R. and Kumari, M. (2000), "Nonsimilar solutions for mixed convection in non-newtonian fluids along a wedge with variable surface heat flux in a porous medium", *J. Porous Media*, Vol. 3 No. 2, pp. 181-184.

Gorla, R.S.R., Chamkha, A.J. and Rashad, A.M. (2011a), "Mixed convective boundary layer flow over a vertical wedge embedded in a porous medium saturated with a nanofluid: natural convection dominated regime", *Nanoscale Research Letters*, Vol. 6 No. 207, pp. 1-9.

Gorla, R.S.R., EL-Kabeir, S.M.M. and Rashad, A.M. (2011b), "Heat transfer in the boundary layer on a stretching circular cylinder in a nanofluid", *Journal of Thermophysics and Heat Transfer*, Vol. 25 No. 1, pp. 183-186.

Ingham, D.B. and Pop, I. (Eds) (2002), "*Transport Phenomena in Porous Media*, Pergamon, Oxford, Vol. II, (2002).

Khan, W.A. and Aziz, A. (2011), "Double-diffusive natural convective boundary layer flow in a porous medium saturated with a nanofluid over a vertical plate: prescribed surface heat, solute and nanoparticle fluxes", *Int. J. Therm. Sci.*, Vol. 50 No. 11, pp. 2154-2160.

Murthy, P.V.S.N., RamReddy, Ch., Chamkha, A.J. and Rashad, A.M. (2013), "Magnetic effect on thermally stratified nanofluid saturated non-darcy porous medium under convective boundary condition", *Int. comm. Heat and Mass Transfer*, Vol. 47, pp. 41-48.

Nadeem, S. and Haq, R.U.I. (2014), "Effect of thermal radiation for megnetohydrodynamic boundary layer flow of a nanofluid past a stretching sheet with convective boundary conditions", *Journal of Computational and Theoretical Nanoscience*, Vol. 11 No. 1, pp. 32-40.

Nadeem, S., Mehmood, R. and Akbar, N.S. (2014), "Optimized analytical solution for oblique flow of a casson-nano fluid with convective boundary conditions", *International Journal of Thermal Sciences*, Vol. 78, pp. 90-100.

Nakayama, A. and Koyama, H. (1991), "Buoyancy induced flow of non-newtonian fluids over a non-isothermal body of arbitrary shape in a fluid-saturated porous medium", *Applied Scientific Research*, Vol. 48 No. 1, pp. 55-70.

Nield, D.A. and Bejan, A. (2006), *Convection in Porous Media*, 3rd ed., Springer, New York, NY.

Nield, D.A. and Kuznetsov, A.V. (2009), "The cheng-minkowycz problem for natural convective boundary layer flow in a porous medium saturated by a nanofluid", *Int. J. Heat Mass Transfer*, Vol. 52 Nos 25-26, pp. 5792-5795.

Pascal, J.P. and Pascal, H. (1997), "Free convection in a non-newtonian fluid saturated porous media with lateral mass flux", *Int. J. Non-Linear Mechanics*, Vol. 32 No. 3, pp. 471-482.

Pop, I. and Ingham, D.B. (2001), *Convective Heat Transfer: Mathematical And Computational Modelling of Viscous Fluids and Porous Media*, Pergamon, Oxford.

RamReddy, C., Murthy, P.V.S.N., Chamkha, A.J. and Rashad, A.M. (2013), "Soret effect on mixed convection flow in a nanofluid under convective boundary condition", *Int. J. Heat and Mass Transfer*, Vol. 64, pp. 384-392.

Rashad, A.M., Abbasbandy, S. and Chamkha, A.J. (2014), "Non-darcy natural convection from a vertical cylinder embedded in a thermally stratified and nanofluid-saturated porous media", *ASME Journal of Heat Transfer*, Vol. 136 No. 2, # 022503 (9 pages), Paper No. HT-13-1078.

Rashad, A.M., EL-Hakiem, M.A. and Abdou, M.M.M. (2011), "Natural convection boundary layer of a non-newtonian fluid about a permeable vertical cone embedded in a porous medium saturated with a nanofluid", *Computers and Mathematics with Applications*, Vol. 62 No. 8, pp. 3140-3151.

Uddin, M.J., Khan, W.A. and Ishmail, A.I.M. (2012), "Free convection boundary layer flow from a heated upward facing horizontal flat plate embedded in a porous medium filled by a nanofluid with convective boundary condition", *Transp. Porous Media*, Vol. 92 No. 3, pp. 867-881.

Vafai, K. (Ed.) (2000), *Handbook of Porous Media*, Marcel Dekker, Marcel.

Yih, K.A. (1998), "Uniform lateral mass flux effect on natural convection of non-newtonian fluids over a cone in porous media", *Int. Comm. Heat mass Transfer*, Vol. 25 No. 7, pp. 959-968.

Further reading

Kelley, C.T. (1995), *Iterative Methods for Linear and Nonlinear Equations*, SIAM, Philadelphia, PA.

Corresponding author

Dr S. Abbasbandy can be contacted at: abbasbandy@yahoo.com